

RESEARCH

Open Access



Potential application of the bulk RNA sequencing in routine MPN clinics

Shenglong Li^{1†}, Sanyun Wu^{2†}, Mingli Xu^{3,4}, Xuedong Li^{3,4}, Xuelan Zuo^{2*} and Yingying Wang^{3,4*} 

Abstract

Background Philadelphia chromosome-negative myeloproliferative neoplasms (MPNs) are chronic hematological malignancies characterized by driver and nondriver mutations, leading to a deregulated immune system with aberrant cytokines and immune cells. Understanding the gene mutation landscape and immune state at various disease stages is crucial for guiding treatment decisions. While advanced techniques like single-cell RNA sequencing and mass cytometry provide valuable insights, their high costs and complexity limit clinical application. In contrast, bulk RNA sequencing (RNA-Seq) offers a cost-effective complementary approach for evaluating genetic mutations and immune profiles.

Methods Peripheral blood and bone marrow samples from treatment-naïve patients diagnosed with polycythemia vera (PV), essential thrombocythemia (ET), and primary myelofibrosis (PMF) were analyzed using RNA sequencing. Additionally, data from the microarray datasets [GSE26049, GSE2191] were included in this study. Bioinformatics methods were employed to interpret gene mutations and immune landscapes in MPN patients.

Results Our findings demonstrate the potential value of RNA-Seq in identifying gene mutations and characterizing the immune profile, including immune cell infiltration, cytokine profiles, and distinct immune-related pathways involved in the development of MPN.

Conclusion Bulk RNA-Seq is a feasible tool for routine clinical practice, providing comprehensive insights into the immune and genetic landscape of MPNs. This approach could enhance personalized treatment strategies and improve prognostic accuracy, ultimately contributing to better management of MPN patients.

Keywords Myeloproliferative neoplasms, Bulk RNA sequencing, Gene mutation, Immune landscape

[†]Shenglong Li and Sanyun Wu contributed equally to this work.

*Correspondence:

Xuelan Zuo
zuoxuelan2004@126.com

Yingying Wang
yingyingvictoria@hotmail.com

¹ Department of Bioinformatics, School of Basic Medical Sciences, Chongqing Medical University, Chongqing 400010, China

² Department of Hematology, Zhongnan Hospital of Wuhan University, Donghu Road, No. 169, Wuhan 430062, China

³ Department of Immunology, School of Basic Medical Sciences, Chongqing Medical University, Chongqing 400010, China

⁴ Chongqing Key Laboratory of Basic and Translational Research of Tumor Immunology, Chongqing Medical University, Chongqing 400010, China

Introduction

Classic myeloproliferative neoplasms (MPNs) are clonal hematopoietic stem cell disorders primarily driven by mutations such as *JAK2V617F*, *MPLW515L/K*, and calreticulin, alongside nondriver mutations like *EZH2*, *ASXL1*, *RAS*, *SRSF2*, *TP53*, and *U2AF1* [1, 2]. These mutations significantly influence disease progression and development. Clinically, MPNs manifest through constitutional symptoms, including fatigue, abdominal discomfort, itching, bone pain, night sweats, and weight loss [3]. Routine blood tests often reveal elevated blood cell counts, while bone marrow examinations confirm malignant hematopoietic stem cell proliferation [4]. Major complications include bleeding and thrombosis,



contributing to high morbidity and mortality rates [5]. A hallmark of MPNs is the chronic inflammatory state characterized by immune dysregulation, abnormal immune cells, and aberrant cytokines [6, 7]. Understanding the interplay between gene mutations and the immune landscape is crucial for guiding treatment decisions and adapting therapies throughout the disease course [8, 9].

Dysregulated cytokines and immune cells play a pivotal role in the pathogenesis and progression of MPNs, particularly PMF. Key cytokines implicated include IL-1 β , TNF- α , IL-6, IL-8, VEGF, PDGF, IFNs, and TGF- β [10–15], with studies highlighting the therapeutic potential of targeting IL-1 β in JAK2-mutated models [16]. Immune cell subsets, such as T-cells (CD4, CD8, Treg, Th1, Th17), NK cells, and myeloid cells (MDSCs, DCs, monocytes, macrophages), are notably dysregulated in MPNs [17–23]. Monocytosis, especially intermediate and non-classical monocytes, is a critical prognostic factor in PMF [24, 25], with increased TNF- α secretion and angiogenic gene expression observed in Tie2+ monocytes [26, 27]. Macrophages, particularly CD68-positive subsets, are significantly elevated in PMF compared to CML, PV, and ET, suggesting their role in bone marrow fibrosis [28]. Transcriptomic analyses further underscore the importance of monocytes and macrophages in MPN pathogenesis, providing insights into potential therapeutic targets [29].

Advanced technologies such as single-cell transcriptomics and mass cytometry have significantly enhanced our understanding of the immune landscape in MPNs [30, 31]. However, these methods are often prohibitively expensive and require specialized expertise, making them difficult to implement in routine clinical practice. Currently, flow cytometry is widely used to assess the phenotypic and functional characteristics of a limited range of immune cell types, but it lacks comprehensiveness [32]. Sanger sequencing and Next-generation DNA sequencing are commonly employed to investigate gene mutations associated with MPNs, but they typically focus on a limited number of genes due to cost constraints. In contrast, bulk RNA sequencing (RNA-Seq) has emerged as a preferred method for comprehensive transcriptome analysis at a relatively low cost. RNA-Seq not only facilitates the discovery of gene expression differences but also offers valuable insights into the immune landscape through bioinformatics tools like CIBERSORTx, which estimates the relative abundance of immune cell types based on gene expression data [33–35]. Recent studies have demonstrated the accuracy of RNA-Seq in interpreting immune cell subsets compared to protein expression evaluated by mass cytometry [36]. This suggests that bulk RNA-Seq can effectively characterize the immune and gene mutation landscape throughout the disease

course, including before treatment, after treatment, and during disease progression. While JAK2 inhibitors have been shown to improve the prognosis for many MPN patients, some individuals do not respond favorably due to severe side effects [37]. Therefore, it is crucial to tailor treatment strategies based on the specific immune and gene mutation profiles of each patient. For certain patients, alternative therapies such as IFN- α or other immune-modulatory drugs may be more appropriate.

This study enrolled treatment-naïve patients diagnosed with PV, ET, and PMF. By analyzing peripheral blood (PB) and bone marrow (BM) samples, the researchers aimed to identify gene mutations and characterize the immune landscape using advanced bioinformatics tools, such as CIBERSORTx for immune cell infiltration analysis. It emphasizes the feasibility of implementing bulk RNA-Seq in routine clinical practice for MPNs, providing valuable insights into the gene mutation landscape and immune characteristics of patients. This approach could enhance personalized treatment strategies and improve prognostic accuracy, ultimately contributing to better management of MPNs. The findings advocate for further validation with larger cohorts and integration of RNA-Seq data into clinical workflows to optimize patient care.

Materials and methods

Patient samples

Three PV patients, 23 ET patients, and 8 PMF patients with confirmed diagnoses without treatment were enrolled in this study. They were treated at the Zhongnan Hospital of Wuhan University between July 1, 2022, and June 30, 2023. Peripheral blood (PB) routine, bone marrow (BM) aspiration and bone biopsy were performed for routine laboratory tests; the residual samples after routine examination of gene mutation and flow cytometry analysis were used further for RNA extraction and RNA sequencing. This study was approved by the Ethics Committee at Zhongnan Hospital of Wuhan University. All methods and procedures associated with this study were conducted following the Good Clinical Practice guidelines and the ethical principles of the Declaration of Helsinki, as well as the local laws.

RNA-sequencing library

The first strand of cDNA was synthesized via the M-MULV reverse transcriptase system. Endogenous RNAs are degraded by RNaseH, and the second strand is synthesized by DNA polymerase I with dNTPs. After purification, the double-stranded cDNA was repaired at the end, followed by the addition of a tail and the connection of sequencing adapters. AMPure XP beads were used to screen cDNAs. PCR amplification was performed, and the PCR products of AMPure XP beads

were again used to purify each cDNA. The shot-gun libraries were sequenced on an Illumina NovaSeq 6000, and paired-end reads of 150 bp were generated.

Comprehensive analysis of immune characteristics

To examine immune cell infiltration in the bone marrow, we utilized CIBERSORTx (<https://cibersortx.stanford.edu>) [33], as described previously, to quantify the infiltration of 22 immune cells and provide an estimation of the abundances of various cell types in a mixed cell population via gene expression data.

Enrichment analysis and correlation analysis

Gene Ontology (GO), Kyoto Encyclopedia of Genes and Genomes (KEGG), and gene set enrichment analysis (GSEA) were implemented via the clusterProfiler package in R v4.3.2. GO terms with adjusted *P* values less than 0.05 were considered significantly enriched in the DEGs. Correlation analysis was implemented with the R packages psych and corrplot.

Weighted gene co-expression network analysis (WGCNA)

WGCNA is a systematic biological approach that enables the characterization of gene association patterns between different samples, with the capacity to identify highly covarying gene sets. In our study, we employed the R package WGCNA to perform WGCNA on MPN bulk RNA-seq data and a microarray dataset. Initially, a suitable soft threshold β was calculated to meet the criteria for constructing a scale-free network. We then transformed the weighted adjacency matrix into a topological overlap matrix (TOM) and calculated the dissimilarity (dissTOM). To perform gene clustering and module identification, we applied the dynamic tree-cut approach. Finally, the modules highly correlated with ET and PMF were identified for subsequent analysis. The R package “linkET” was used to perform Mantel test analysis between the MPN subtypes (PV, ET, PMF) and gene sets in WGCNA.

Gene mutation analysis

In this study, we used spliced transcript alignment to a reference (STAR) and the Genome Analysis Toolkit (GATK) to perform gene mutation analysis. The detailed analysis process is described on GATK’s official website (<https://gatk.broadinstitute.org/hc/enus/categories/360002302312>). To investigate the mutations associated with MPNs, we utilized the R package “maftools” to generate waterfall plots and a Lollipop chart, which displays mutation landscapes in MPN patients.

Statistical analysis

Trimmomatic and fastp were used for the preprocessing of the raw RNA-Seq reads. Clean reads were mapped to human reference genome sequences (GRCh38) via HISAT2 with the GRCh38/V34 annotation file in Gencode (<https://www.encodegenes.org/human/>). The read count matrix was obtained by using the feature count. The rank-in strategy described previously [38] (<http://www.badd-cao.net/rank-in/index.html>) was used to remove the batch effects between the bulk RNA-Seq data and the microarray dataset. PCA plots were subsequently generated with the Factoextra package and FactoMineR package [39, 40]. The limma package in R v4.3.2 was used to process the expression matrix and identify the DEGs among BMs (PV, ET, and PMF), following the standard analysis process [$|\log(\text{FC})| > 2$ and adjusted *P* value < 0.05 , $|\log(\text{FC})| > 4$ for significant DEGs]. Heatmaps were generated with the pheatmap package, and volcano plots were generated with the ggplot2 and ggVolcano packages. Protein–protein interaction (PPI) analysis was performed via the Search Tool for the Retrieval of Interacting Genes/Proteins (STRING) database (<https://cn.string-db.org>) and Cytoscape software.

Data access

The data generated in this paper have been deposited in the OMIX, China National Center for Bioinformation / Beijing Institute of Genomics, Chinese Academy of Sciences under the accession no. OMIX008313 (<https://ngdc.cnbc.ac.cn/omix/view/OMIX008313>). The microarray datasets [GSE26049, GSE2191] of patients with MPN and HCs [PV_PB (*n* = 41), ET_PB (*n* = 19), PMF_PB (*n* = 9), HC_PB (*n* = 21), HC_BM (*n* = 4)] from the GEO database were retrieved.

Results

Patient characteristics

Five peripheral blood (PB) and 30 bone marrow (BM) samples from 34 patients without treatment, including 3 PV patients, 23 ET patients, and 8 PMF patients, were used for bulk RNA-Seq. The baseline features of these patients are detailed in Table 1. Three patients were diagnosed with triple negative; one patient presented with *CALR* mutation; and the remaining patients carried the *JAK2V617F* mutation. Among these treatment-naïve patients, blood test results were missing for 6 outpatients. Leucocytosis (leukocytes $\geq 10 \times 10^9/\text{L}$) was observed in 15/28 patients, and elevated lactate dehydrogenase (LDH) levels were observed in 14/21 patients. Additionally, 4 ET patients whose Next-generation DNA Sequencing results revealed gene mutations, such as *JAK2V617F*, *ASXL1*, *TET2*, *EPPK1*, and *CSMD1*, are shown in Supplementary Table S1.

Table 1 Clinical features of MPN patients

ID	Gender	Age (Years)	Source of sample	Driver gene mutation	JAK2V617F Mutation burden	LDH(IU/mL)	W77 expression (WT1/10 ⁴ copies ABL1)	WBC (10 ⁹ /L)	HGB(g/L)	PLT(10 ¹² /L)
PV1	M	75	BM	JAK2	78.77%	246	0.20%	17.23	177.8	631
PV2	F	59	BM	JAK2	53.44%	337	0.39%	10.01	173.1	543
PV3	M	67	BM	JAK2	10.8%	NA	0.16%	NA	NA	NA
ET1	M	52	BM	JAK2	12.73%	NA	0.23%	NA	NA	NA
ET2	F	55	BM	Triple negative	NA	138	0.06%	8.2	111	889
ET3	M	52	BM	JAK2	20.55%	154	0.20%	6.75	144.3	694
ET4	F	75	BM	JAK2	21.58%	269	0.02%	10.2	123	612
ET5	F	68	BM	Triple negative	NA	NA	0.02%	NA	NA	NA
ET6	F	78	BM	JAK2	6.23%	193	0.26%	6.3	130.6	576
PBET1	F	87	PB	JAK2	10.47%	NA	0	NA	NA	NA
PBET2	M	66	PB	JAK2	0.01%	NA	0	6.62	111.5	426
ET7	M	67	BM	JAK2	4.32%	181	0.09%	7.93	50.3	745
ET8	F	63	BM/PB	JAK2	7.50%	NA	0.11%	5.8	124	554
ET9	M	35	BM	JAK2	22.7%	311	0.001	13.5	159	613
ET10	F	56	BM/PB	JAK2	0.02%	NA	0	7.24	142.3	490
ET11	M	76	BM	JAK2	35.11%	248	0.15%	10.4	132	647
ET12	F	65	BM	CALR	0	350	0.14%	14.43	126	1948
ET13	M	74	BM	JAK2	32.49%	277	0	11.6	90	1235
ET14	M	70	BM	JAK2	71.53%	531	1.93	20.83	183	822
ET15	F	72	BM	JAK2	7.04%	183	0.31%	6.45	182	633
ET16	F	57	BM	Triple negative	NA	282	NA	10.02	141	547
PBET3	F	52	PB	JAK2	4.07%	NA	0	7.59	143	566
PBET4	M	33	PB	JAK2	2.55%	NA	0	9.83	162	561
ET17	M	74	BM	JAK2	39.30%	389	0.03%	12	126	689
ET18	M	74	BM	JAK2	11.14%	171	0.07%	10.6	118	869
ET19	F	58	BM	JAK2	37.34%	293	0.26%	7.9	129	836
PMF1	M	56	BM	JAK2	75.99%	NA	0.41%	16.87	93.6	883
PMF2	M	64	BM	JAK2	57.70%	234	0.15%	15	173	501
PMF3	M	66	BM	JAK2	73.30%	252	1.99%	11	62	251
PMF4	M	64	BM	JAK2	13.35%	NA	0.07%	NA	NA	NA
PMF5	M	57	BM	JAK2	43.99%	280	0.69%	10.16	76.9	522
PMF6	M	48	BM	JAK2	90.87%	437	3.06%	14.63	159.5	241
PMF7	M	80	BM	JAK2	72.29%	NA	5.51%	NA	NA	NA
PMF8	M	65	BM	JAK2	97.60%	NA	1.34%	9.7	89	408

LDH Lactate dehydrogenase, W77 Wilms tumor gene 1, WBC White blood cell, HGB Hemoglobin, PLT Platelet, F Female, M Male, PB Peripheral blood, BM Bone marrow, NA Not available

Gene mutations in MPNs evaluated with RNA-Seq data

Gene mutations were identified in PV, ET, and PMF according to mutation type, mutation variation classification, and mutation burden (Supplementary Fig. S1). Frequent driver gene mutations and nondriver mutations, such as those in *TP53*, *JAK2*, *ASXL1*, *EZH2*, *EPPK1*, and *MPL*, are shown in Fig. 1. *JAK2* mutations were detected in all 3 PV patients. Moreover, two patients presented with multihit *JAK2* mutations, as indicated in black (Fig. 1A). For 19 ET patients, *JAK2* mutations were detected in 13/19 patients, *ASXL1* mutations were detected in 4/19 patients, and *EPPK1* mutations were detected in 3/19 patients (Fig. 1C). Moreover, NGS results from 4 ET patients confirmed *EPPK1* mutations or *ASXL1*, which was also detected via the transcriptome (Supplementary Table S1). Among the 8 PMF patients, 7 presented with *JAK2* mutations, 6 presented with *ASXL1* mutations, and 1 patient presented with an *EPPK1* mutation (Fig. 1B). *TP53* gene mutations, specifically p.P33R (25/30), p.R205P (1/30), and p.R141H (1/30), were identified in MPNs. Analysis of their clinical significance using the IARC TP53 Database (<http://p53.iarc.fr>) revealed that p.R205P and p.R141H are pathogenic, while p.P33R is classified as benign. Missense mutation and frame-shift-ins mutation were the major types of these genes in the MPNs. Mutation loci were also identified, as demonstrated with the Lollipop chart in Fig. 1D, for *TP53* and *JAK2*, and most mutations tended to converge at several loci. More examples of gene mutations, such as those in *TP53*, *JAK2*, *ASXL1*, and *EPPK1*, are shown in Supplementary Fig. S2A, S2B, and S2C for PV, ET, and PMF, respectively.

Differential immune gene expression and prominent immune pathways implicated in MPNs

Thirty-five samples from 34 patients were sequenced, including 5 PB samples and 30 BM samples (3 PV, 19 ET, and 8 PMF samples). Since very few PB samples were included in our cohort, 90 PB samples from datasets (GSE26049), including 21 healthy controls, 41 PV, 19 ET, and 9 PMF samples, were used for gene differential expression analysis, and another 4 microarray datasets of healthy BM controls from GSE2191 were also included in the analysis. Therefore, a total of 129 samples were included in this study. The whole sample was well differentiated by cluster analysis (Supplementary Fig. S3A) after removing the batch effect via the rank-in method. The PCA results revealed that the gene expression features of the three MPN subtypes from PB and BM could be distinguished from those from PB and BM in the healthy control group (Supplementary Fig. S3B), and the features from PB were also very different from those

from BM. As indicated in Fig. 2A, ET and PMF presented some common gene expression features because there are overlapping features between the later stage of ET and the early stage of PMF; even in the clinic, it is difficult to make a differential diagnosis between ET and overt PMF. Compared with those of HCs, each MPN subtype presented approximately 700–800 significantly differentially expressed genes (DEGs); among these genes, 620 DEGs were common to PV, ET, and PMF (Fig. 2B), which is likely related to MPNs. The immune-related genes among the DEGs are indicated in the heatmap (Fig. 2C). These immune-related genes were subsequently subjected to Kyoto Encyclopedia of Genes and Genomes (KEGG) pathway enrichment analysis, and the results suggested that the common pathways of PV, ET and PMF, such as the NF-Kappa B signaling pathway, Th 17 cell differentiation, Th1 and Th2 cell differentiation, NK cell-mediated cytotoxicity, MAPK, cytokine–cytokine receptor interaction and antigen processing and presentation, are potentially involved in MPN development. There were also several differential pathways among these three entities, such as the IL17 and B-cell receptor signaling pathways, which were enriched only in the PV, the Toll-like receptor signaling pathway was enriched more in the PV and ET, and the Ras and Rap1 signaling pathways were enriched only in the PMF (Fig. 2D). There were unique immune-related features for each MPN subtype, which was confirmed by KEGG and GO pathway analysis (Supplementary Fig. S4).

MPN-related immune gene traits evaluated by transcription

To explore the associations between immune traits and disease subtypes, WGCNA was used to identify modules of highly correlated genes and to investigate the relationships between these modules and MPN subtypes. All these genes were separated into 43 different gene modules by hierarchical clustering (Supplementary Fig. S5), and each module is presented in an individual color, as indicated in Fig. 3A. On the basis of correlation analysis (Supplementary Fig. S6), several disease-related trait modules associated with PV, ET, and PMF with different grades of correlations were identified. The modules therein, which presented a high correlation with both PMF and ET, were labeled module complex 1 (MC1: red box) and module complex 2 (MC2: blue box) in Fig. 3A. MC1 was positively correlated with PMF and negatively correlated with ET. MC2, in contrast, was negatively correlated with PMF and positively correlated with ET. Furthermore, the Mantel test results (Fig. 3B) revealed that all the modules in MC1 and MC2 were strongly correlated with the PMF and ET subtypes, and most of the

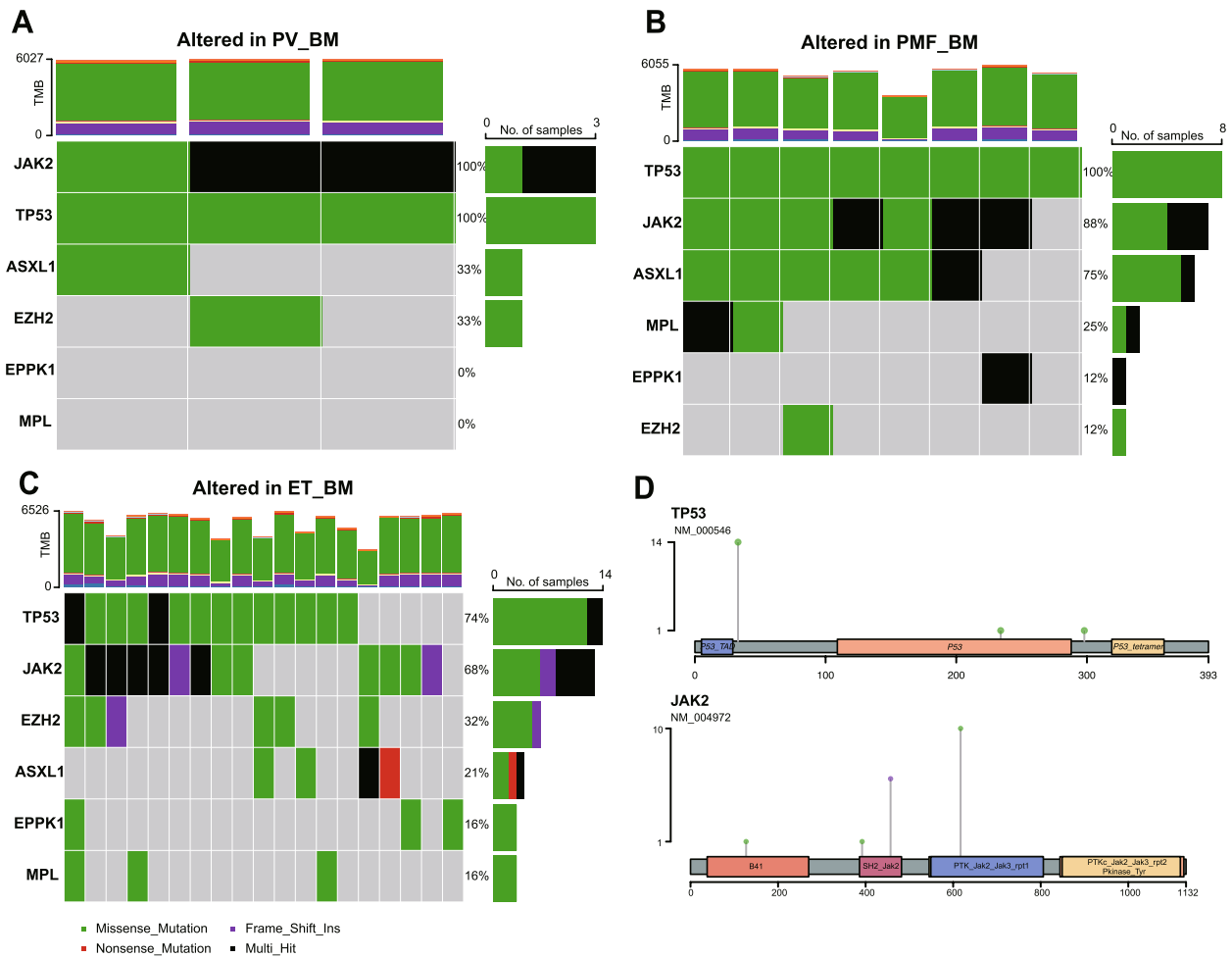


Fig. 1 Gene mutations identified by RNA-seq in MPNs. **A, B, C** Examples of mutation types for several genes, such as *TP53*, *JAK2*, *ASXL1*, *MPL*, *EZH2*, and *EPPK1*, in PV_BM, PMF_BM, and ET_BM, respectively. **D** Lollipop chart of the mutation loci for *TP53* and *JAK2* in ET

modules presented a certain degree of correlation with PV.

Further analysis was performed with genes included in MC1 and MC2 to explore PMF and ET particular immune traits. A heatmap of immune genes, including those in MC1, is presented in Fig. 4A. GO enrichment analysis identified five groups of genes that were potentially related to disease: positive regulation of cytokine production, chemotaxis, taxis, response to molecules of bacterial origin, and cell killing (Fig. 4B). Important signaling pathways, including the cytokine–cytokine receptor interaction, acute myeloid leukemia, Toll–like receptor, and TNF signaling pathways, were enriched via KEGG analysis (Fig. 4C). Gene correlation analysis revealed correlations among the 46 top genes, such as *IL4R*, *IL17RB*, *IFNARI*, *CXCL10*, and *CXCL16* (Fig. 4D). To uncover the interaction between proteins encoded by these 46 genes,

the STRING database was utilized to perform the analysis. Ten hub genes of MC1 genes were obtained via the cytoHubba plugin from the PPI network (Fig. 4E): *MPO*, *ICAM1*, *RENT*, *CTSG*, *RNASE3*, *RNASE2*, *LTF*, *LCN2*, *ELANE*, and *CAMP*.

Similar analysis procedures were performed with genes in MC2. The heatmap of immune gene expression in the three MPN subtypes presented different colors, which reflected the relative expression of each gene (Fig. 5A). GO enrichment analysis revealed that the above genes are involved mainly in immune functions, such as leukocyte proliferation, including lymphocyte and mononuclear cell proliferation; the regulation of leukocyte proliferation; and the extrinsic apoptotic signaling pathway (Fig. 5B). Furthermore, pathways related to cytokine–cytokine interactions, the PI3K–Akt signaling pathway, acute myeloid leukemia, and Th 17 cell differentiation

were enriched via KEGG analysis (Fig. 5C). Correlation analysis also revealed good correlations among these genes. PPI network analysis revealed the top 10 hub genes: *CD48*, *KRAS*, *IL2RA*, *CD27*, *FAS*, *IL6ST*, *MAVS*, *CYBB*, *NFKB1*, and *PAK1*.

Immune cell compositions and cytokine gene expression levels in MPNs evaluated by transcriptional analysis

CIBRSORTx was used to delineate the transcriptome matrix and translate it into the abundance of immune cell subsets in the bone marrow and peripheral blood from different groups. As shown in Fig. 6, a comprehensive analysis of immune cell subsets, including T cells, B cells, monocytes, NK cells, Treg cells, neutrophils, and other cells, could be performed with gene expression data. Compared with those in healthy BM, the frequencies of naïve B cells, naïve CD4+ T cells, CD4+ Treg cells, CD8+ T cells, and monocytes were lower. Moreover, a significantly increased frequency of memory resting CD4 T cells, resting NK cells,

eosinophils, and neutrophils was observed in the three MPN subtypes (Fig. 6). In PB, a decreased frequency of naïve B cells and an increased frequency of eosinophils were significantly different from those in healthy PB. However, in contrast to that observed in the BM, a significantly decreased frequency of resting memory CD4 T cells was identified. A slight increase in the frequency of monocytes was observed in PMF compared with PV and ET, but this difference was not significant (Supplementary Fig. S7).

Dysregulated cytokines are a major feature of MPN. Major immune cytokine genes, such as *IL-4*, *IL-6*, *IL-2*, *IFNG*, *CSF1R*, *EPO*, and *CCR1*, were included among the immune genes, as demonstrated with heatmaps (Fig. 2C). Cytokines can be divided into several groups, such as the interleukin family, colony-stimulating factors, growth factors, and tumor necrosis factors. Each group of cytokine-related gene expression levels could also be explored as indicated in Supplementary Fig. S8.

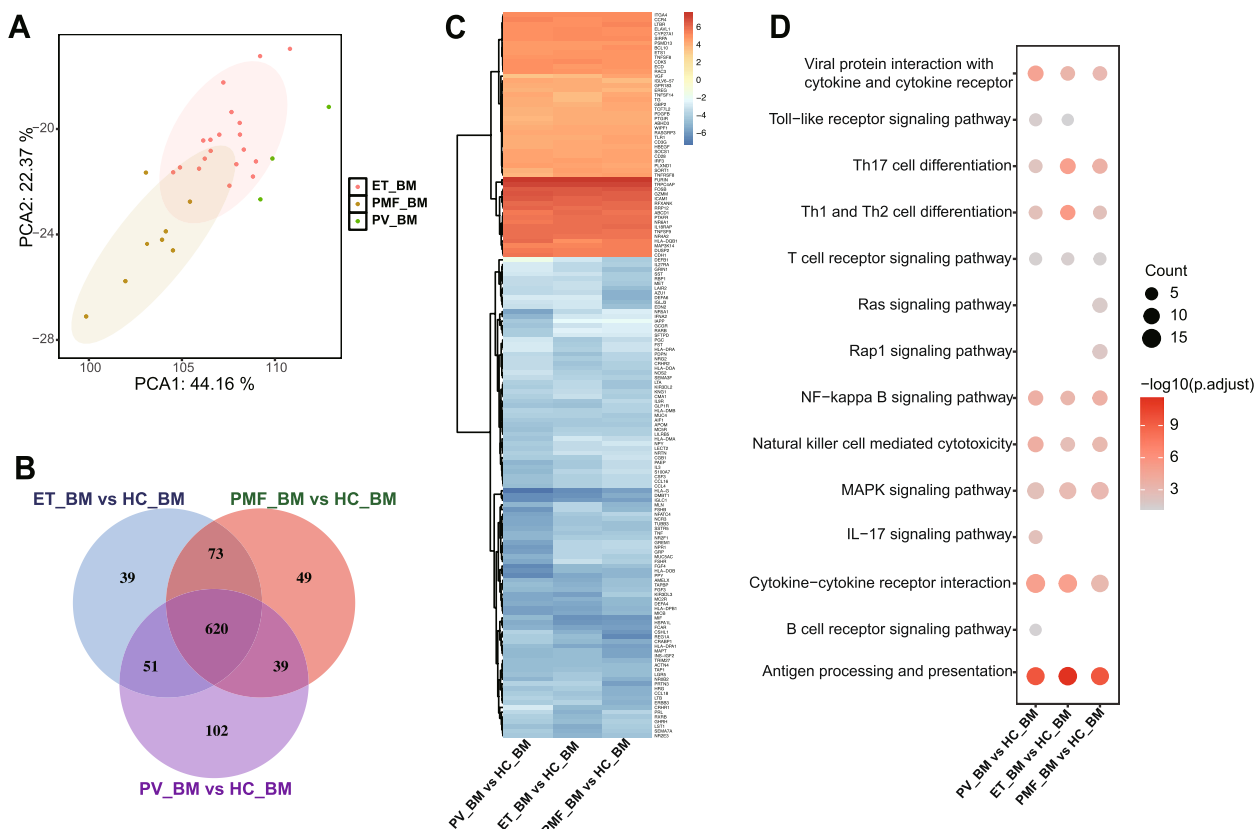


Fig. 2 Immune genes and pathways in MPNs. **A** PCA diagram after removing the batch effect for all samples from PV_BM, ET_BM, and PMF_BM. **B** Venn diagram of DEGs between each MPN subtype and HCs. **C** Heatmap of significant DEGs between each MPN subtype and HCs. **D** Immune-related pathways identified via KEGG analysis in each MPN subtype compared with HCs. The size of the dots represents the $-\log_{10}$ (adjusted *p* value)

Discussion

In summary, this study aimed to explore the potential of bulk RNA-Seq in identifying gene mutations and the immune landscape in MPNs. Our results highlight the feasibility of incorporating bulk RNA-Seq into routine clinical practice, providing comprehensive insights into gene mutations and immune pathways implicated in MPNs. However, further validation with larger sample sizes and in-depth analyses of the correlations between gene mutations and immune traits is needed.

Previous research utilizing RNA microarrays and chips on PB and BM samples has demonstrated differential gene expression in MPNs, underlining the importance of RNA-Seq for identifying MPN-related genes and pathways [41–43]. Transcriptomic analyses of specific cell types such as monocytes, macrophages, granulocytes, platelets, and CD34+ cells have revealed mechanisms involved in MPN development [29, 44–47]. Additionally, detailed studies using single-cell RNA-Seq of CD34+ hematopoietic stem cells have shed light on their role in MPN initiation [48–51]. Collectively, these findings suggest that the transcriptome of MPNs may clarify underlying mechanisms of disease progression.

Bulk RNA-Seq can effectively detect various gene mutations including type, classification, burden, and loci offering valuable insights into the mutation landscape of MPN patients [34]. Its high performance and low cost make bulk RNA-Seq an attractive complementary approach to current Sanger DNA sequencing for investigating gene mutations, as Sanger sequencing typically focuses on hotspot regions of genes rather than analyzing the entire gene. For instance, in our cohort, 7 out of 8 PMF patients had *ASXL1* mutations, which are often overlooked in routine clinical practice but are critical for prognosis. *ASXL1* mutations promote fibrosis and lead to poor outcomes in PMF patients [52, 53]. Furthermore, identifying multiple hit genes through bulk RNA-Seq may elucidate the limited efficacy of JAK2 inhibitors in certain patients, making it possible to construct a detailed gene mutation landscape for MPNs in clinical settings. However, the gene mutations identified through RNA-Seq require further confirmation by DNA sequencing, as these mutations are predominantly single nucleotide polymorphisms (SNPs) that may not necessarily be pathogenic. For example, the frequency of *TP53* mutations was found to be significantly higher

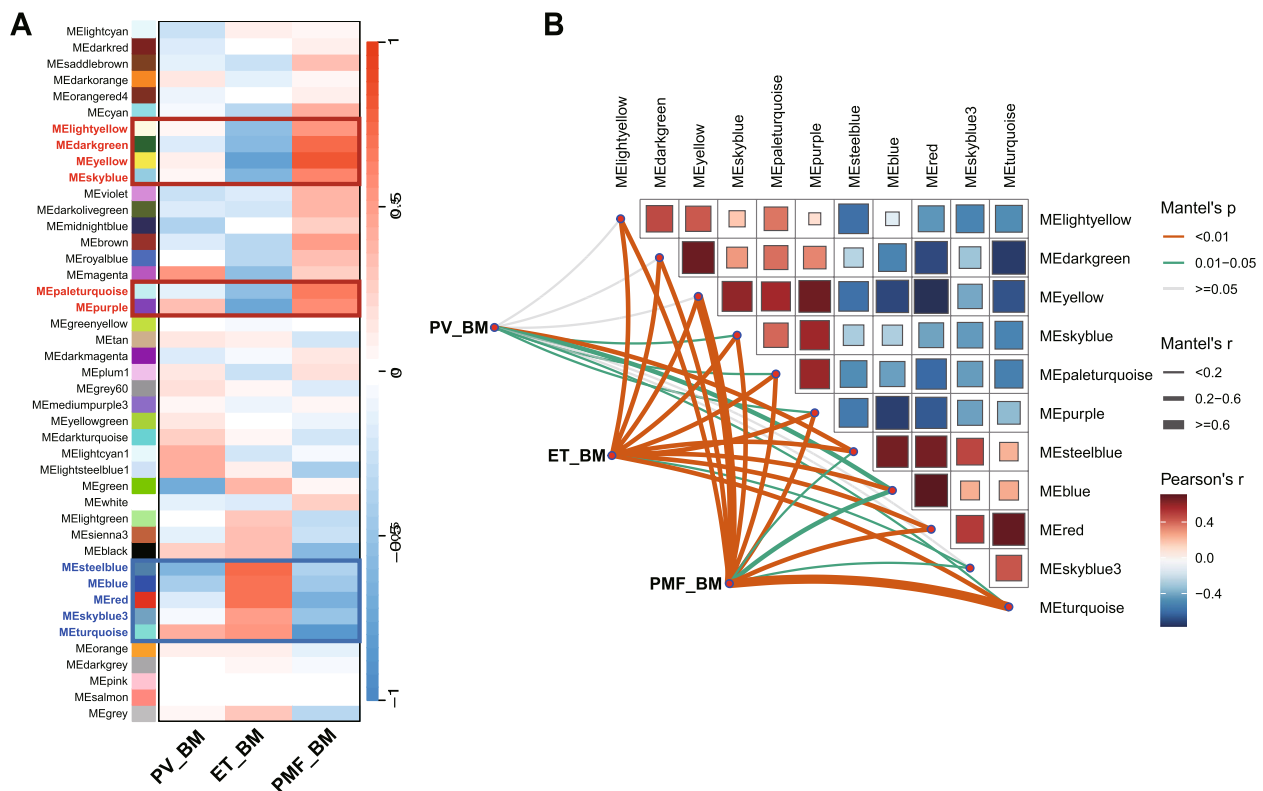


Fig. 3 Immune gene traits associated with MPNs. **A** WGCNA of gene expression; the gene modules in the red box are labeled MC1, and the gene modules in the blue box are labeled MC2. **B** Mantel test analysis between the MPN subtypes (PV, ET, PMF) and gene modules in MC1 and MC2. The color of the line reflects the *P* value, and the thickness of the line reflects the correlation *r* value. The color of the square reflects whether there is a positive or negative correlation between two modules; red indicates a positive correlation, and blue indicates a negative correlation

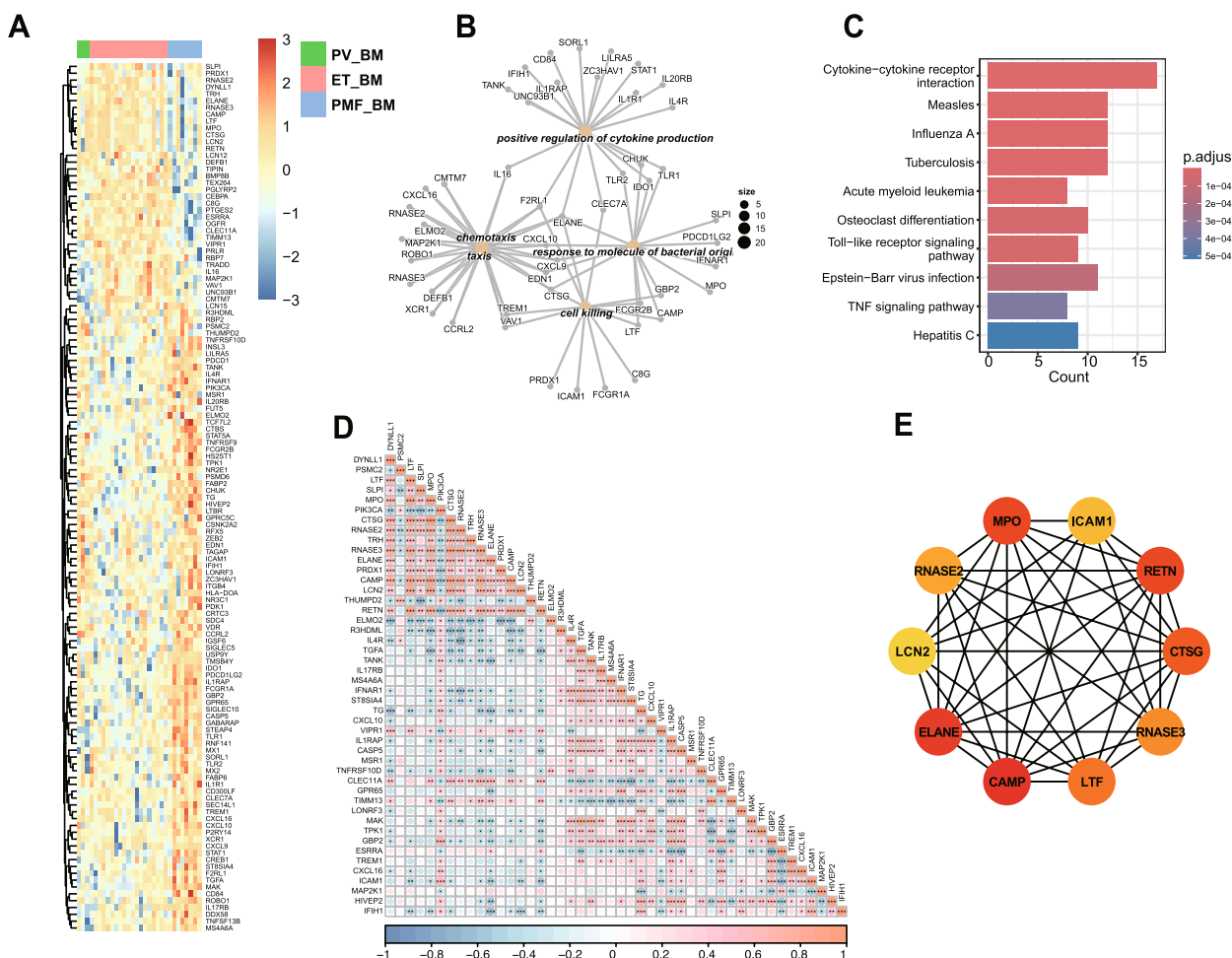


Fig. 4 Features of immune genes included in MC1. **A** Heatmaps of immune genes in MC1. **B** GO enrichment analysis of immune genes in MC1. **C** Immune-related pathways from KEGG analysis of immune genes in MC1. **D** Correlation analysis of immune genes in MC1; red indicates positive, and blue indicates negative. A dark color represents a strong correlation; a light color represents a weak correlation. **E** Top 10 hub genes from the PPI network analysis for the genes included in MC1. Nodes denote encoded proteins, and edges denote interactions between encoded proteins. The color represents the scores ranked by the MCC methods. A deeper color denotes more important genes with higher scores

in transcriptional analysis compared to the 16.1% (less than 25%) reported in studies using DNA sequencing [54, 55]. After cross-referencing these mutations with *TP53* databases, only two patients were found to carry *TP53* mutations of pathogenic significance, representing a frequency of 6.7% (2/30) [56]. These mutations identified through RNA-seq should be carefully interpreted by assessing their clinical significance using databases such as COSMIC or ClinVar to confirm their specificity. Given that current clinical DNA sequencing primarily targets hotspot regions of genes, which may miss certain mutations, the value of RNA-seq in identifying gene mutations should be emphasized. RNA-seq is particularly valuable for detecting splicing variants

and fusion genes, which are often overlooked in traditional DNA sequencing.

Considering MPNs are chronic inflammatory diseases with dysregulated immune systems, monitoring the immune state is crucial throughout disease progression. Currently, flow cytometry and ELISA kits evaluate immune cell subsets and cytokine levels, respectively, but these methods provide limited insights. While advanced techniques like mass cytometry and single-cell RNA-Seq are useful, their high costs and accessibility issues hinder widespread use. Thus, Bulk RNA-seq offers several key advantages in studying the immune landscape of MPNs. First, it provides comprehensive transcriptome coverage, capturing a global view of gene expression that includes both immune and non-immune components. This allows

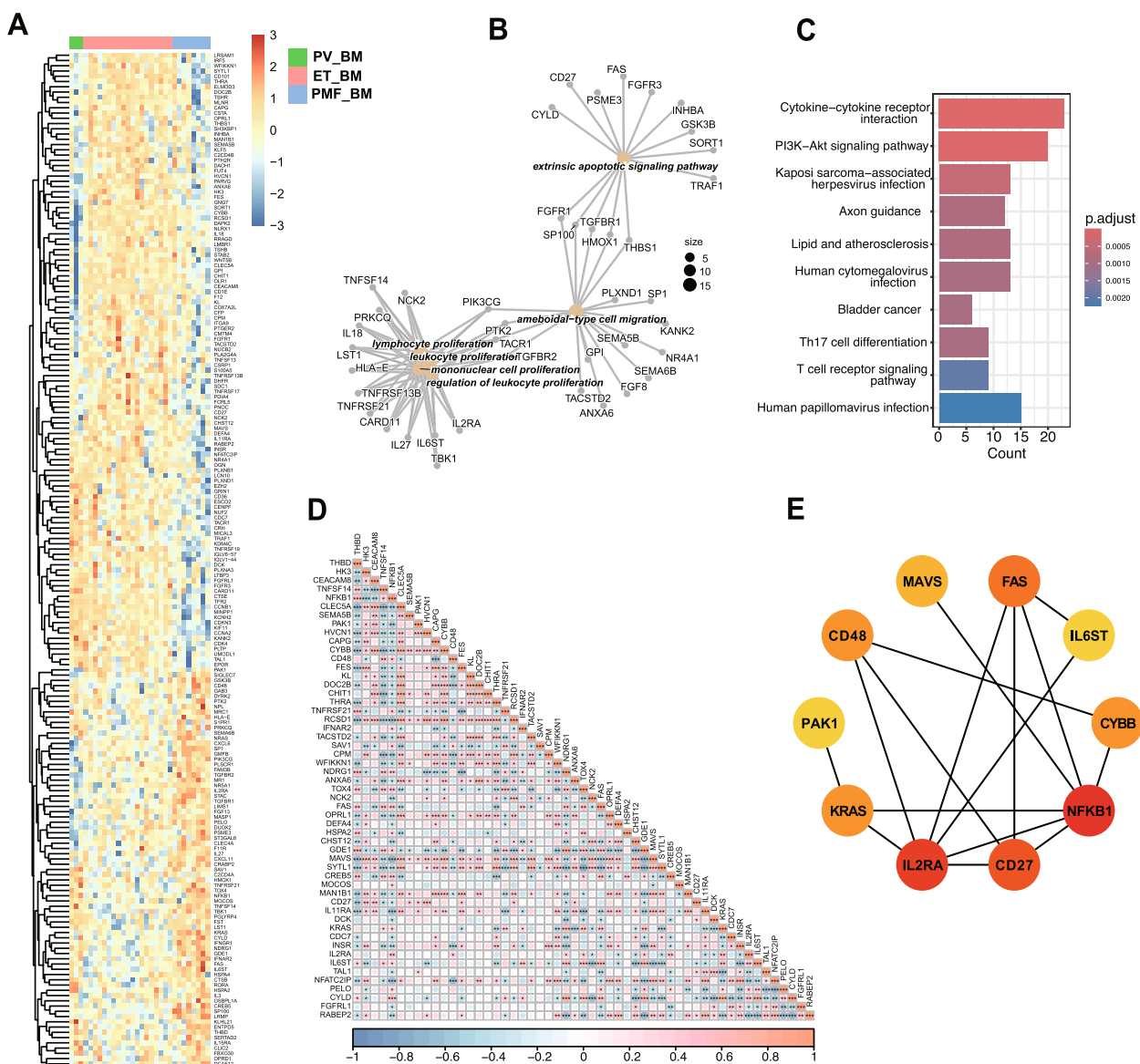


Fig. 5 Features of immune genes included in MC2. **A** Heatmaps of immune genes in MC2. **B** GO enrichment analysis of immune genes in MC2. **C** Immune-related pathways from KEGG analysis of immune genes in MC2. **D** Correlation analysis of immune genes in MC2; red indicates positive, and blue indicates negative. A dark color represents a strong correlation; a light color represents a weak correlation. **E** Top 10 hub genes from the PPI network analysis for the genes included in MC2. Nodes denote encoded proteins, and edges denote interactions between encoded proteins. The color represents the scores ranked by the MCC methods. A deeper color denotes more important genes with higher scores

for the quantification of cytokines, chemokines, and other immune-related genes, revealing the immune and inflammatory status of the MPNs [57]. Second, computational deconvolution tools like CIBERSORT enable the estimation of immune and stromal cell proportions, facilitating the characterization of immune cell infiltration, such as T cells, macrophages, and dendritic cells [58]. Third, it is cost-effective and scalable, making it suitable for tracking systematically changes in immune signatures,

including analyses at different time points before and after treatment, thereby better detecting changes in the body’s immune status and treatment responses.

Baseline immune features can guide personalized therapies, such as IFN therapy for active IFN signaling or JAK2/NF-κB inhibitors for hyperactive JAK-STAT/NF-κB pathways. Dynamic RNA-Seq monitoring at various time points enables the evaluation of therapeutic

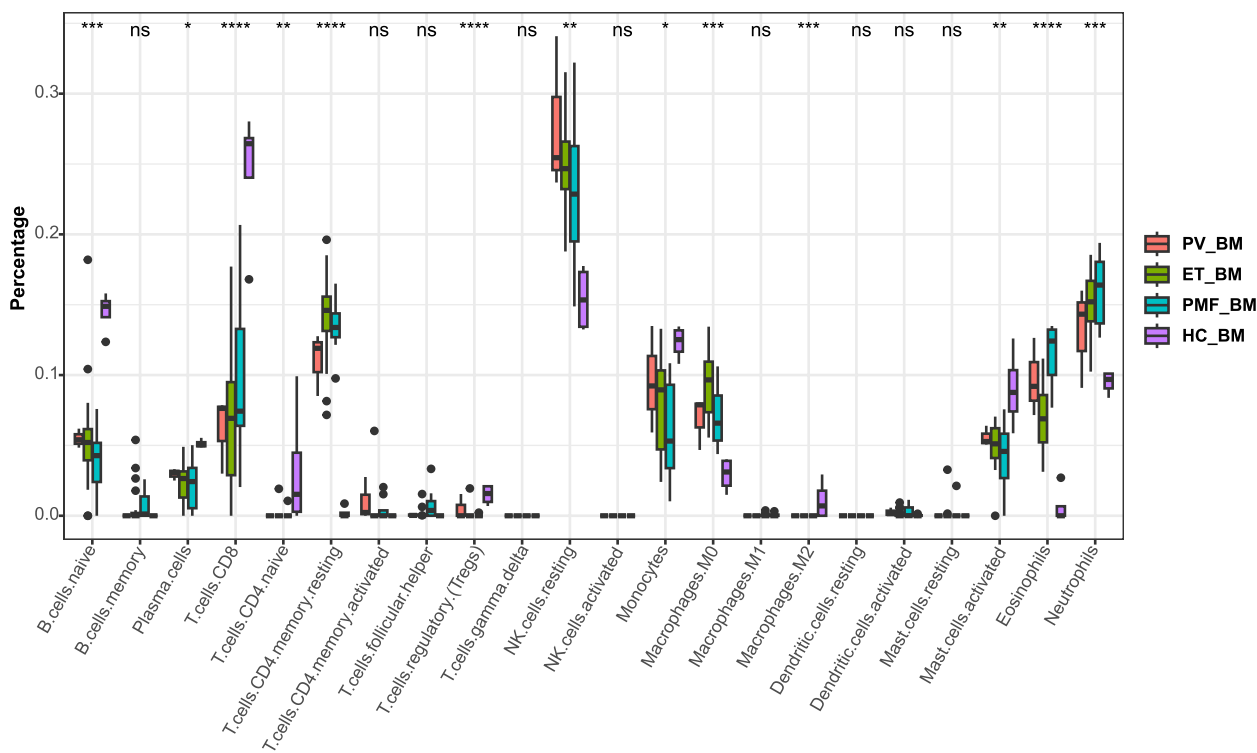


Fig. 6 Immune cell subsets evaluated with CIBERSORTx for PV_BM, ET_BM, PMF_BM, and HC_BM. (* indicates $P \leq 0.05$; ** indicates $P \leq 0.01$; *** indicates $P \leq 0.001$; ns, no significance)

efficacy and the tailoring of interventions based on immune variations. Importantly, for patients on long-term JAK2 inhibitor therapy, RNA-Seq can detect early immune suppression, facilitating timely switches to alternative therapies to restore immune function and reduce infection risks. This precision approach enhances patient safety and optimizes therapeutic outcomes by aligning treatments with individual immune dynamics.

In conclusion, the systematic evaluation of immune landscape changes and gene mutation variations throughout the entire disease cycle is crucial in managing MPNs. Bulk RNA-Seq offers significant advantages for monitoring the evolution of MPNs by simultaneously providing data on gene mutations and immune landscape variations at a low cost. It could support personalized and precision medicine, ultimately enhancing the management of MPNs and improving patient outcomes. Its implementation in clinical settings is highly feasible, requiring minimal sample input and offering an affordable cost. However, RNA-Seq has notable limitations. First, it measures gene expression and functional insights, which may not always align with protein expression and function. Second, accurate interpretation of RNA-Seq data requires expertise in genetic, immunology and bioinformatics to avoid overinterpretation or misleading conclusions. Therefore, validation with large

clinical samples and high-dimensional technologies such as mass cytometry and single-cell sequencing is essential to ensure the accuracy of transcriptome interpretations. Integrating matched data into an artificial intelligence learning system could further enhance the accuracy of interpreting gene mutations and immune landscapes derived from bulk RNA-Seq. Additionally, developing an online tool for interpreting raw transcriptome data would be beneficial. With advancements in translational medicine and bioinformatics, bulk RNA-Seq has the potential to deliver more precise genetic and immune insights for MPN patients, positioning it as a valuable complementary tool alongside current approaches in routine clinical practice.

Supplementary Information

The online version contains supplementary material available at <https://doi.org/10.1186/s12885-025-13947-x>.

Supplementary Material 1: Supplementary Fig. S1. Gene mutations identified by RNA-seq in MPNs. (A) Gene variation type, variation classification, and top 10 mutated genes in ET. (B) Gene variation type, variation classification, and top 10 mutated genes in PV. (C) Gene variation type, variation classification, and top 10 mutated genes in PMF.

Supplementary Material 2: Supplementary Fig. S2. Mutation landscape of four genes in MPN subtypes. (A) Lollipop chart of the mutation loci of *TP53*, *JAK2*, and *ASXL1* in the PV. (B) Lollipop chart of the mutation loci of

TP53, *JAK2*, *ASXL1*, and *EPPK1* in ET. (C) Lollipop chart of the mutation loci of *TP53*, *JAK2*, *ASXL1*, and *EPPK1* in PMF.

Supplementary Material 3: Supplementary Fig. S3. Clustering analysis between MPN and healthy control samples. (A) The gene cluster for different MPNs and healthy controls. Platform 1 included 30 BM samples and 5 PB samples, Platform 2 included 91 samples, and Platform 3 included 4 healthy BM samples from another dataset. Each color represents one group of samples. (B) PCA diagram after removing the batch effect for all the samples described previously, including MPN_BM, HC_BM, MPN_PB, and HC_PB.

Supplementary Material 4: Supplementary Fig. S4. GO and KEGG analyses of immune genes with differential expression between each subtype of MPN. (A) Differential immune pathways identified by KEGG analysis between ET_BM and PMF_BM; ET_BM and PV_BM; PMF_BM and PV_BM. (B) Comparison of major immune functions identified by GO analysis between ET_BM and PMF_BM; ET_BM and PV_BM; PMF_BM and PV_BM. The size of the dots represents the number of genes. The color of the dots denotes the adjusted *p* value.

Supplementary Material 5: Supplementary Fig. S5. WGCNA showing the co-expression module in MPNs. (A) Dendrogram of the gene clusters. (B) Heatmaps of selected immune genes.

Supplementary Material 6: Supplementary Fig. S6. Correlation analysis between immune gene modules and MPN subtypes.

Supplementary Material 7: Supplementary Fig. S7. Immune cell subsets evaluated with CIBERSORTx for PV_PB, ET_PB, PMF_PB, and HC_PB. (* indicates $P \leq 0.05$; ** indicates $P \leq 0.01$; *** indicates $P \leq 0.001$; ns, no significance).

Supplementary Material 8: Supplementary Fig. S8. Heatmaps of cytokine gene expression in MPN subtypes. (A) Heatmaps of major IL family gene expression. (B) Heatmaps of major chemokine family gene expression. (C) Heatmaps of major colony-stimulating factor gene expression. (D) Heatmaps of major growth factor gene expression. (E) Heatmaps of the gene expression of *TNFA* and its receptors *TNFRSF1A* and *TNFRSF1B*.

Acknowledgements

We thank all the patients for their approval in providing their residual samples for this research.

Authors' contributions

Y-Y.W: Main researcher and primary writer of the manuscript. S-L.L: Conducted the analysis of the RNA transcriptome, contributed to the writing of the Materials and Methods section and also prepared the figures. S-Y.W: Collected clinical samples and data, and performed RNA extraction and sequencing and wrote part of the Materials and Methods section. M-L.X and X-D.L: Responsible for creating tables and arranging references. X-L.Z: Planned and supervised the study.

Funding

This work was supported by the National Natural Science Foundation of China (82000135) and the National Science Foundation of Chongqing City (CSTB2023NSCQ-MSX0241).

Data availability

The data generated in this paper have been deposited in the OMIX, China National Center for Bioinformatics / Beijing Institute of Genomics, Chinese Academy of Sciences under the accession no. OMIX008313 (<https://ngdc.cncb.ac.cn/omix/view/OMIX008313>). The microarray datasets [GSE26049, GSE2191] included in this study were retrieved from the GEO database.

Declarations

Ethics approval and consent to participate

This study was reviewed and approved by Zhongnan Hospital of Wuhan University in Wuhan, Hubei Province, China (2021-066). Informed consent to participate was obtained from all the participants in the study when they did the bone marrow aspiration.

Consent for publication

Not applicable.

Competing interests

The authors declare no competing interests.

Received: 3 December 2024 Accepted: 17 March 2025

Published online: 22 April 2025

References

- Thiele J, Kvasnicka HM, Orazi A, Gianelli U, Gangat N, et al. The international consensus classification of myeloid neoplasms and acute Leukemias: myeloproliferative neoplasms. *American J Hematol*. 2023;98(1):166–79.
- Luque Paz D, Kralovics R, Skoda RC. Genetic basis and molecular profiling in myeloproliferative neoplasms. *Blood*. 2023;141(16):1909–21.
- Tremblay D, Mesa R. Addressing symptom burden in myeloproliferative neoplasms. *Best Pract Res Clin Hematol*. 2022;35(2):101372.1.
- Barbui T, Thiele J, Gisslinger H, Kvasnicka HM, Vannucchi AM, et al. The 2016 WHO classification and diagnostic criteria for myeloproliferative neoplasms: document summary and in-depth discussion. *Blood Cancer J*. 2018;8(2):15.
- Greenfield G, McMullin MF. A spotlight on the management of complications associated with myeloproliferative neoplasms: a clinician's perspective. *Expert Rev Hematol*. 2018;11(1):25–35.
- Strickland M, Quek L, Psaila B. The immune landscape in BCR-ABL negative myeloproliferative neoplasms: inflammation, infections, and opportunities for immunotherapy. *Br J Hematol*. 2022;196(5):1149–58.
- Geyer HL, Dueck AC, Scherber RM, Mesa RA. Impact of Inflammation on Myeloproliferative Neoplasm Symptom Development. *Mediators Inflamm*. 2015;2015:1–9.
- Romano M, Sollazzo D, Trabaneli S, Barone M, Polverelli N, Perricone M, et al. (2017) Mutations in *JAK2* and *Calreticulin* genes are associated with specific alterations of the immune system in myelofibrosis. *Onc Immunology*. 2017;6(10):e1345402.
- Hermouet S. Mutations, inflammation and phenotype of myeloproliferative neoplasms. *Front Oncol*. 2023;22(13):1196817.
- Masselli E, Pozzi G, Gobbi G, Merighi S, Gessi S, Vitale M, Carubbi C. Cytokine Profiling in Myeloproliferative Neoplasms: Overview on Phenotype Correlation, Outcome Prediction, and Role of Genetic Variants. *Cells*. 2020;9(9):2136.
- Wang Y, Zuo X. Cytokines frequently implicated in myeloproliferative neoplasms. *Cytokine X*. 2019;1(1):100005.
- Rahman MFU, Yang Y, Le BT, Dutta A, Posyniak J, Faughnan P, et al. Interleukin-1 contributes to clonal expansion and progression of bone marrow fibrosis in JAK2V617F-induced myeloproliferative neoplasm. *Nat Commun*. 2022;13(1):5347.
- Lai HY, Brooks SA, Craver BM, Morse SJ, Nguyen TK, Haghghi N, Garbati MR, Fleischman AG. Defective negative regulation of Toll-like receptor signaling leads to excessive TNF- α in myeloproliferative neoplasms. *Blood Adv*. 2019;3(2):122–31.
- Dunbar A, Kim D, Lu M, Farina M, Bowman RL, Yang JL, et al. CXCL8/CXCR2 signaling mediates bone marrow fibrosis and represents a therapeutic target in myelofibrosis. *Blood*. 2023;141(20):2508–2519.15.
- Agarwal A, Morrone K, Bartenstein M, Zhao ZJ, Verma A, Goel S. Bone marrow fibrosis in primary myelofibrosis: pathogenic mechanisms and the role of TGF- β . *Stem Cell Investig*. 2016;26(3):5.
- Rai S, Grockowiak E, Hansen N, Luque Paz D, Stoll CB, Hao-Shen H, et al. Inhibition of interleukin-1 β reduces myelofibrosis and osteosclerosis in mice with JAK2-V617F driver myeloproliferative neoplasm. *Nat Commun*. 2022;13(1):5346.
- Veletic I, Prijic S, Manshour T, Noguera-Gonzalez GM, Verstovsek S, et al. Altered T-cell subset repertoire affects treatment outcome of patients with myelofibrosis. *Hematol*. 2020;106(9):2384–96.
- Riley CH, Jensen MK, Brimnes MK, Hasselbalch HC, Bjerrum OW, Straten P, et al. Increase in circulating CD4+CD25+Foxp3+ T cells in patients with Philadelphia-negative chronic myeloproliferative neoplasms during treatment with IFN- α . *Blood*. 2011;118(8):2170–3.

19. Massa M, Rosti V, Campanelli R, Fois G, Barosi G. Rapid and long-lasting decrease of T-regulatory cells in patients with myelofibrosis treated with ruxolitinib. *Leukemia*. 2014;28(2):449–51.
20. Naismith E, Steichen J, Sopper S, Wolf D. NK Cells in Myeloproliferative Neoplasms (MPN). *Cancers (Basel)*. 2021;13(17):4400.
21. Wang JC, Kundra A, Andrei M, Baptiste S, Chen C, Wong C, et al. Myeloid-derived suppressor cells in patients with myeloproliferative neoplasm. *Leuk Res*. 2016;43:39–43.
22. Veletic I, Manshoury T, Multani AS, Yin CC, Chen L, Verstovsek S, et al. Myelofibrosis osteoclasts are clonal and functionally impaired. *Blood*. 2019;133(21):2320–4.
23. Fowles JS, Fisher DAC, Zhou A, Oh ST. Altered Dynamics of Monocyte Subpopulations and Pro-Inflammatory Signaling Pathways in Polycythemia Vera Revealed By Mass Cytometry. *Blood*. 2019;134(Supplement_1):4210–4210.
24. Tefferi A, Shah S, Mudireddy M, Lasho TL, Barraco D, et al. Monocytosis is a powerful and independent predictor of inferior survival in primary myelofibrosis. *Br J Hematol*. 2018;183(5):835–8.
25. Morsia E, Gangat N. Myeloproliferative Neoplasms with Monocytosis. *Curr Hematol Malig Rep*. 2022;17(1):46–51.
26. Barone M, Catani L, Ricci F, Romano M, Forte D, Auteri G, et al. The role of circulating monocytes and JAK inhibition in the infectious-driver inflammatory response of myelofibrosis. *Oncolmmunology*. 2020;9(11):1782575.
27. Maekawa T, Kato S, Kawamura T, Takada K, Sone T, Ogata H, et al. Increased SLAMF7high monocytes in myelofibrosis patients harboring JAK2V617F provide a therapeutic target of elotuzumab. *Blood*. 2019;134(10):814–25. <https://doi.org/10.1182/blood.2019000051>.
28. Molitor DCA, Boor P, Bunes A, Schneider RK, Teichmann LL, Körber RM, et al. Macrophage frequency in the bone marrow correlates with morphologic subtype of myeloproliferative neoplasm. *Ann Hematol*. 2021;100(1):97–104.
29. Fan W, Cao W, Shi J, Gao F, Wang M, Xu L, et al. Contributions of bone marrow monocytes/macrophages in myeloproliferative neoplasms with JAK2V617F mutation. *Ann Hematol*. 2023;102(7):1745–59.
30. Zavidij O, Haradhvala NJ, Meyer R, Cui J, Verstovsek S, Oh S, et al. MPN-238 Single-Cell RNA Profiling of Myelofibrosis Patients Reveals Pelabresib-Induced Decrease of Megakaryocytic Progenitors and Normalization of CD4+ T Cells in Peripheral Blood. *Clin Lymphoma Myeloma Leuk*. 2022;22:S331–2.
31. Fisher DAC, Miner CA, Engle EK, Hu H, Collins TB, et al. Cytokine production in myelofibrosis exhibits differential responsiveness to JAK-STAT, MAP kinase, and NFκB signaling. *Leukemia*. 2019;33(8):1978–95.
32. O'Sullivan JM, Mead AJ, Psaila B. Single-cell methods in myeloproliferative neoplasms: old questions, new technologies. *Blood*. 2023;141(4):380–90.
33. Steen CB, Liu CL, Alizadeh AA, Newman AM. Profiling Cell Type Abundance and Expression in Bulk Tissues with CIBERSORTx. *Methods Mol Biol*. 2020;2117:135–57.
34. Schischlik F, Jäger R, Rosebrock F, Hug E, Schuster M, Holly R, et al. Mutational landscape of the transcriptome offers putative targets for immunotherapy of myeloproliferative neoplasms. *Blood*. 2019;134(2):199–210.
35. Schischlik F. Transcriptional configurations of myeloproliferative neoplasms. *Int Rev Cell Mol Biol*. 2022;366:25–39.
36. Oetjen KA, Lindblad KE, Goswami M, Gui G, Dagur PK, et al. Human bone marrow assessment by single-cell RNA sequencing, mass cytometry, and flow cytometry. *JCI Insight*. 2018;3(23):e124928.
37. Duminuco A, Torre E, Palumbo GA, Harrison C. A Journey Through JAK Inhibitors for the Treatment of Myeloproliferative Diseases. *Curr Hematol Malig Rep*. 2023;18(5):176–89.
38. Tang K, Ji X, Zhou M, Deng Z, Huang Y, Zheng G, et al. Rank-in: enabling integrative analysis across microarray and RNA-seq for cancer. *Nucleic Acids Res*. 2021;49(17):e99–e99.
39. Kassambara A, and Mundt F. Factoextra: Extract and Visualize the Results of Multivariate Data Analyses. 2020. Available at <https://CRAN.R-project.org/package=factoextra>.
40. Lê S, Josse J, Husson F. FactoMineR: An R Package for multivariate analysis. *J Stat Softw*. 2008;25(1):1–18. <https://doi.org/10.18637/jss.v025.i01>.
41. Hasselbalch HC, Thomassen M, Hasselbalch Riley C, Kjær L, Stauffer Larsen T, et al. Whole Blood Transcriptional Profiling Reveals Deregulation of Oxidative and Antioxidative Defense Genes in Myelofibrosis and Related Neoplasms. Potential Implications of Nrf2 Downregulation for Genomic Instability and Disease Progression. Mills K, editor. *PLoS ONE*. 2014;9(11):e112786.
42. Skov V, Thomassen M, Kjær L, Larsen MK, Knudsen TA, Ellervik C, et al. Whole blood transcriptional profiling reveals highly deregulated atherosclerosis genes in Philadelphia-chromosome negative myeloproliferative neoplasms. *Eur J Hematol*. 2023;111(5):805–14.
43. Wong WJ, Baltay M, Getz A, Fuhrman K, Aster JC, Hasserjian RP, et al. Gene expression profiling distinguishes prefibrotic from overtly fibrotic myeloproliferative neoplasms and identifies disease subsets with distinct inflammatory signatures. Bunting KD, editor. *PLoS ONE*. 2019;14(5):e0216810.
44. Rampal R, Al-Shahrour F, Abdel-Wahab O, Patel JP, Brunel JP, et al. Integrated genomic analysis illustrates the central role of JAK-STAT pathway activation in myeloproliferative neoplasm pathogenesis. *Blood*. 2014;123(22):e123–33.
45. Shen Z, Du W, Perkins C, Fechter L, Natu V, et al. Platelet transcriptome identifies progressive markers and potential therapeutic targets in chronic myeloproliferative neoplasms. *Cell Rep Med*. 2021;2(10):100425.
46. Baumeister J, Maié T, Chatain N, Gan L, Weinbergerova B, de Toledo MAS, et al. Early and late stage MPN patients show distinct gene expression profiles in CD34+ cells. *Ann Hematol*. 2021;100(12):2943–56.
47. Guijarro-Hernández A, Vizmanos JL. Transcriptomic comparison of bone marrow CD34+ cells and peripheral blood neutrophils from ET patients with JAK2 or CALR mutations. *BMC Genom Data*. 2023;24(1):40.
48. Van Egeren D, Kamaz B, Liu S, Nguyen M, Reilly CR, Kalyva M, et al. Transcriptional differences between JAK2-V617F and wild-type bone marrow cells in patients with myeloproliferative neoplasms. *Exp Hematol*. 2022;107:14–9.
49. Tong J, Sun T, Ma S, Zhao Y, Ju M, et al. Hematopoietic Stem Cell Heterogeneity Is Linked to the Initiation and Therapeutic Response of Myeloproliferative Neoplasms. *Cell Stem Cell*. 2021;28(3):502–513.e6.
50. Hsu CC, Chen YJ, Huang CE, Wu YY, Wang MC, et al. Molecular heterogeneity unravelled by single-cell transcriptomics in patients with essential thrombocythaemia. *Br J Hematol*. 2020;188(5):707–22.
51. Psaila B, Wang G, Rodriguez-Meira A, Li R, Heuston EF, Murphy L, et al. Single-Cell Analyses Reveal Megakaryocyte-Biased Hematopoiesis in Myelofibrosis and Identify Mutant Clone-Specific Targets. *Mol Cell*. 2020;78(3):477–92.
52. Shi Z, Liu J, Zhao Y, Yang L, Cai Y, et al. ASXL1 mutations accelerate bone marrow fibrosis via EGR1-TNFA axis-mediated neoplastic fibrocyte generation in myeloproliferative neoplasms. *Hematologica*. 2023;108(5):1359–73.
53. Wang Z, Liu W, Wang M, Li Y, Wang X, et al. Prognostic value of ASXL1 mutations in patients with primary myelofibrosis and its relationship with clinical features: a meta-analysis. *Ann Hematol*. 2021;100(2):465–79.
54. Walter W, Nadarajah N, Hutter S, Müller H, Haferlach C, et al. Characterization of myeloproliferative neoplasms based on genetics only and prognostication of transformation to blast phase. *Leukemia*. 2024;38(12):2644–52.
55. Kubesova B, Pavlova S, Malcikova J, Kabathova J, Radova L, et al. Low-burden TP53 mutations in chronic phase of myeloproliferative neoplasms: association with age, hydroxyurea administration, disease type and JAK2 mutational status. *Leukemia*. 2018;32(2):450–61.
56. Bouaoun L, Sonkin D, Ardin M, Hollstein M, Byrnes G, et al. TP53 Variations in Human Cancers: New Lessons from the IARC TP53 Database and Genomics Data. *Hum Mutat*. 2016;37(9):865–76.
57. Thorsson V, Gibbs DL, Brown SD, Wolf D, Bortone DS, et al. The Immune Landscape of Cancer. *Immunity*. 2018;48(4):812–830.e14.
58. Finotello F, Trajanoski Z. Quantifying tumor-infiltrating immune cells from transcriptomics data. *Cancer Immunol Immunother*. 2018;67(7):1031–40.

Publisher's Note

Springer Nature remains neutral with regard to jurisdictional claims in published maps and institutional affiliations.